

# Using Anatomical Human Body Model for FEM SAR Simulation of a 3T MRI System



Alexander Prokop, Tilmann Wittig, and Abhay Morey

## 1 Introduction

Specific absorption rate (SAR), the dissipated power per tissue mass, is used to quantify the human exposure to electromagnetic fields in frequency ranges between 100 kHz and 6 GHz. To approximate the temperature rise distribution, it is usually averaged over masses of 1 g (SAR-1g) or 10 g. The averaging procedure to be used after computational determination of the electromagnetic fields using the finite difference time domain (FDTD) method or finite integration theory (FIT) in rectangular hexahedral grid meshes has been defined in the IEC/IEEE 62704-1 standard [1].

However, with the finite element method (FEM), electromagnetic fields are usually calculated on unstructured, i.e. tetrahedral or curved element meshes, for which the 62704-1 averaging procedure is not directly applicable. Therefore, in the IEC/IEEE 62704-4 standard [2], an iterative sampling procedure has been defined. Its output can be used with the 62704-1 averaging procedure.

In the following, we show how this sampling procedure, which was developed for the standard application to wireless communication devices, is also applicable to other field distributions from devices like magnetic resonance imaging (MRI) systems for which SAR is also an essential quantity to evaluate patient safety.

---

A. Prokop (✉) · T. Wittig  
Dassault Systèmes SIMULIA, Darmstadt, Germany  
e-mail: [alexander.prokop@3ds.com](mailto:alexander.prokop@3ds.com)

A. Morey  
Dassault Systèmes SIMULIA, Pune, India

## 2 Simulation Setup

A generic MRI RF coil for 3 Tesla resonating at 128 MHz is simulated in full 3D together with an anatomically correct human body model (HBM), the Female Visible Human [3, 4]; tissue properties are based on the typical Gabriel [5] parameters with background tissue modelled as fat (Fig. 1). Coil capacitors are represented by ports in the 3D model, so the coil can easily be tuned by an EM-circuit co-simulation in post-processing. During the full simulation run, a relatively coarse mesh is sufficient, as no details of the HBM need to be resolved. The resulting fields are recorded on a Huygens box enclosing the HBM.

As a next step, the obtained fields are used as an equivalent field source (EFS) for a simulation where only the human body model is contained. Agreement of the results with the full simulation have been verified as presented in [6]. The EFS has been applied for both FIT hexahedral time domain simulation with a 2-mm mesh step and a FEM frequency domain simulation with a mesh of about 1 million tetrahedra.

SAR-1g has been calculated for FIT on the 2-mm discretization mesh and with different sampling steps for FEM, scaled to an accepted power of 1 W.

As an initial sampling step, 62704-4 [2] suggests to stay below the cubic root of the quotient of the averaging mass divided by the maximum occurring mass density, in our case  $2000 \text{ kg/m}^3$  for bone resulting in a maximum initial mesh step of 7.94 mm. We choose an initial mesh step of 5 mm.

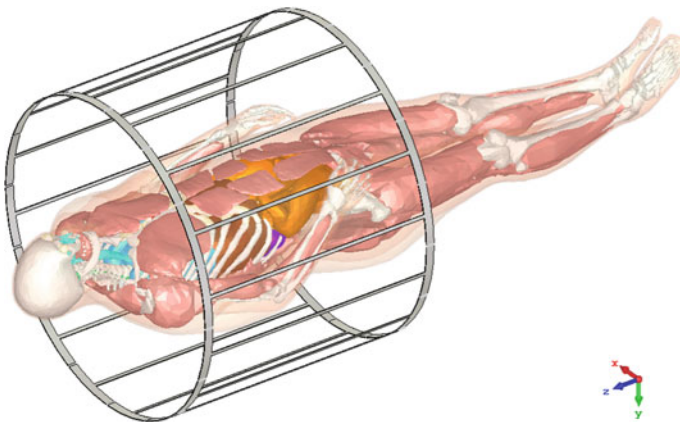


**Fig. 1** MRI coil setup with HBM

### 3 Results

The following figures show the SAR-1g distributions in coronal cross sections. With 5-mm sampling, the maximum SAR-1g is 0.264 W/kg. Figure 2a shows the plane with the maximum; see the red spot between stomach and intestine. With 2-mm sampling, maximum SAR-1g is 0.37 W/kg, but at a different location. Figure 2b

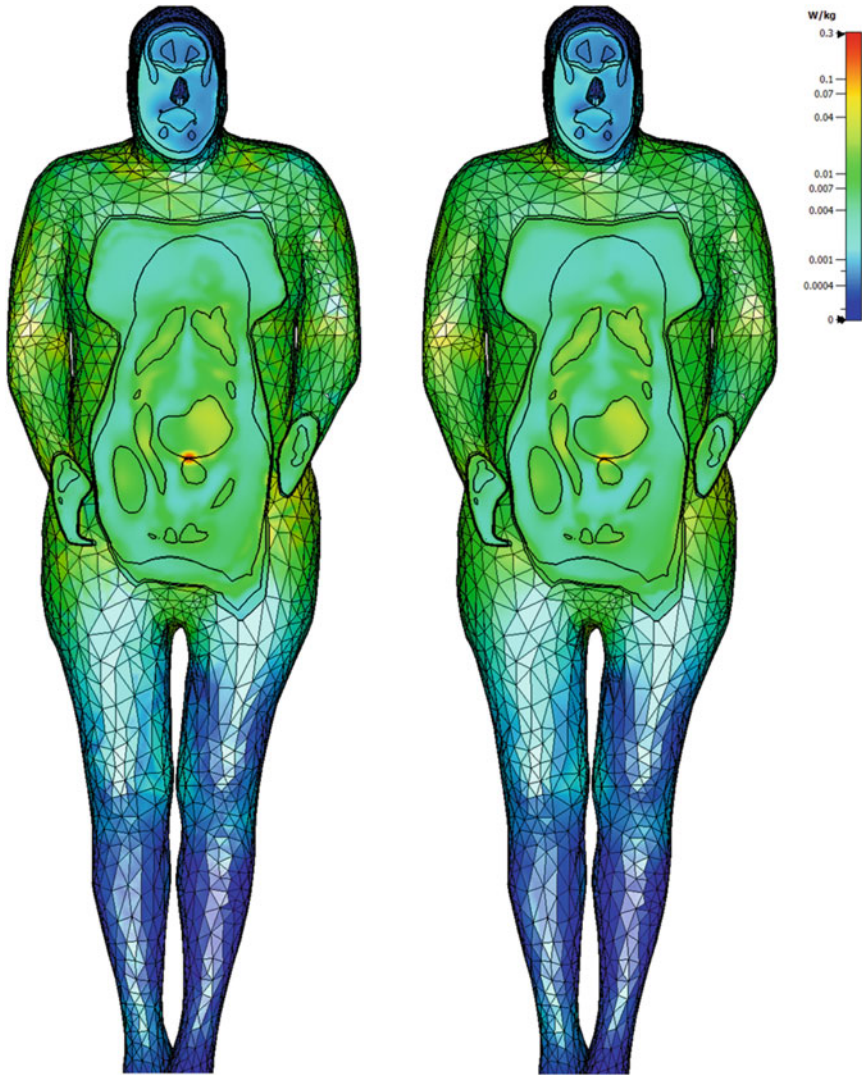


**Fig. 2** (a) left: SAR-1g with 5-mm sampling at  $y = -65$ ; (b) right: SAR-1g with 2-mm sampling at  $y = -65$

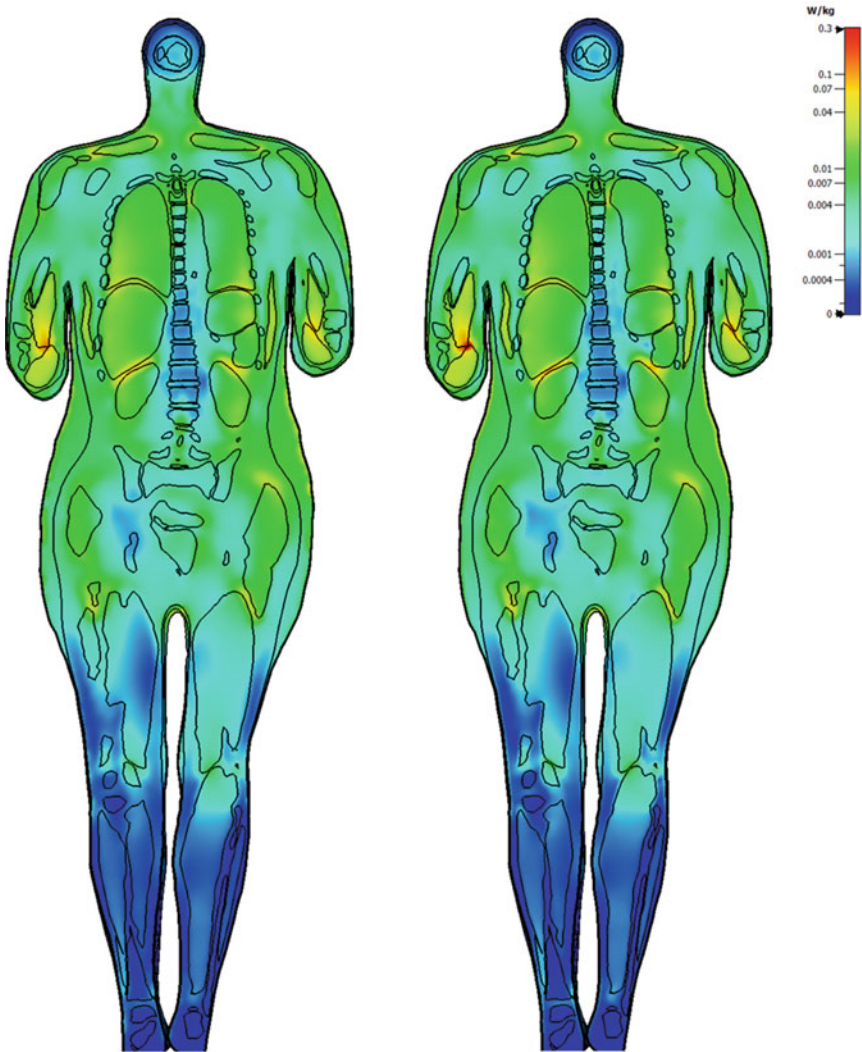
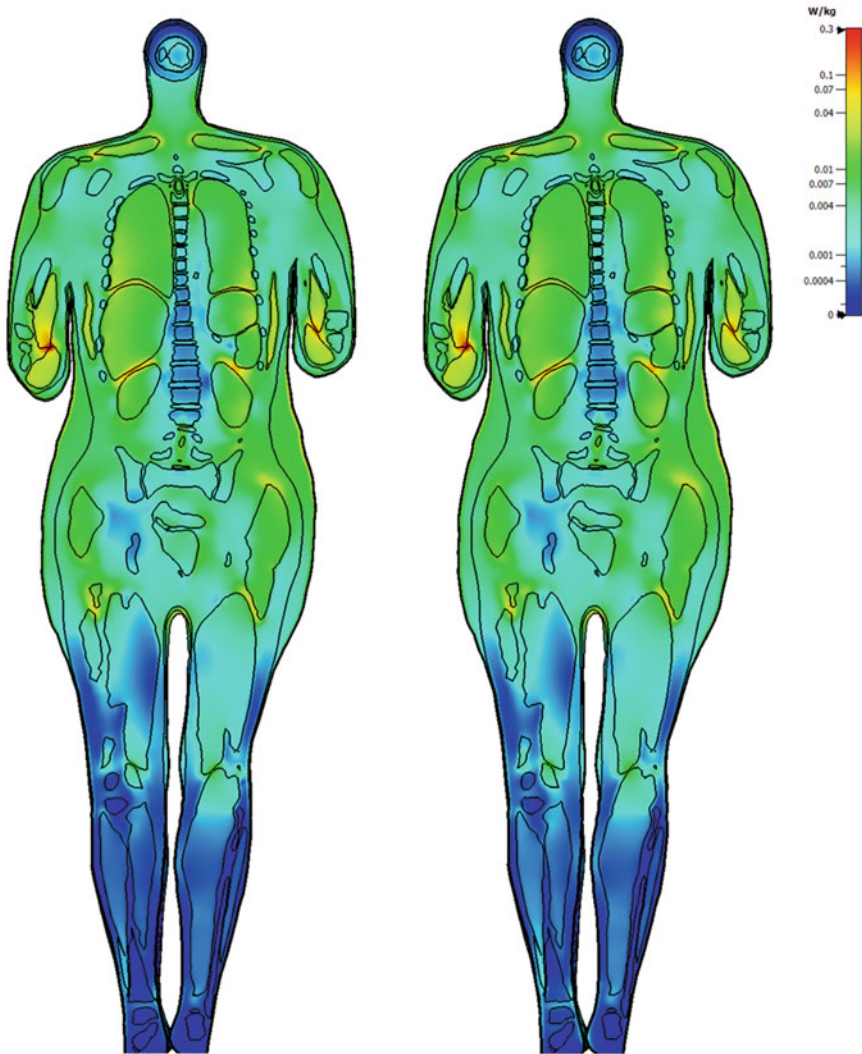


**Fig. 3** (a) left: SAR-1g with 5-mm sampling at  $y = 63$ ; (b) right: SAR-1g with 2-mm sampling at  $y = 63$

shows only a small rise at the stomach/intestine spot. In Figs. 3a and 3b, we see the actual maximum SAR-1g position in the right arm, where the 5-mm sampling results shown in Fig. 3a only have a local maximum of 0.123 W/kg.

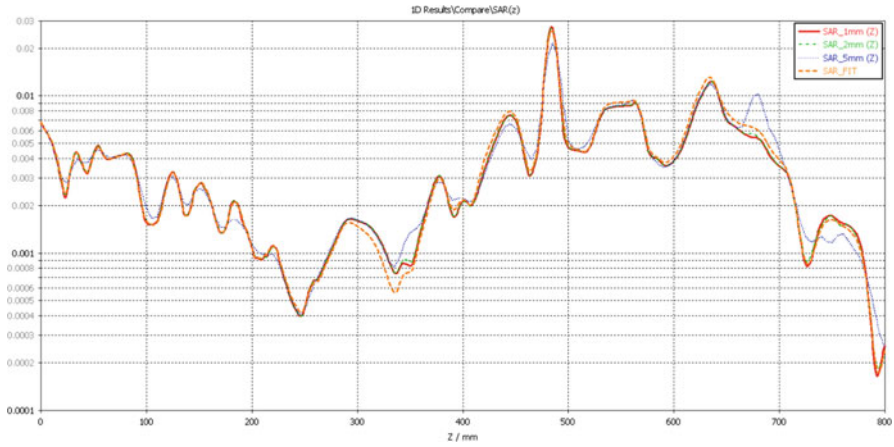
Figures 4a and 4b show a good agreement of the 1-mm sampling (0.341 W/kg) and the FIT results (0.338 W/kg) for maximum SAR-1g in value and location.

Figure 5 compares FEM SAR-1g with different sampling steps to FIT SAR-1g along the line shown dashed in Fig. 6.



**Fig. 4** (a) left: SAR-1g with 1-mm sampling at  $y = 63$ ; (b) right: SAR-1g from FIT according to 62704-1 at  $y = 63$

As in Fig. 2a, the 5-mm sampling shows a peak around  $z = 680$  mm, which does not exist in the finer sampling and the FIT results. There are some minor deviations of the 1-mm and 2-mm sampling results from FIT with reasonable relative error or in regions where SAR is very low.



**Fig. 5** FEM SAR-1g for different sampling steps with FIT SAR-1 g compared along a line through  $x = 30, y = 50$

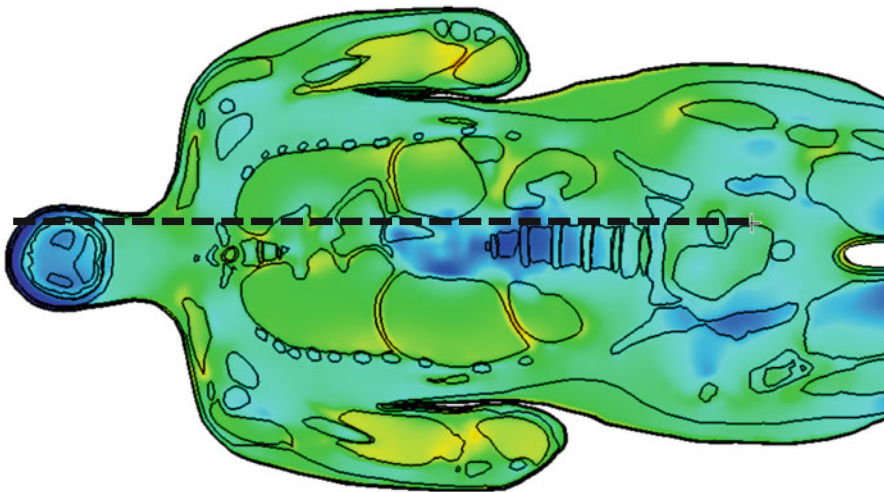


**Fig. 6** Dashed line used for comparison in plane  $y = 50$

### 4 SAR Profiles

Figures 7, 8, and 9 show the maximum SAR-1g per plane for each coordinate direction, i.e., Fig. 7 shows the maximum SAR-1g in each sagittal plane at coordinates  $x$  from  $-250$  to  $250$  (right to left body part), clearly showing the maximum in

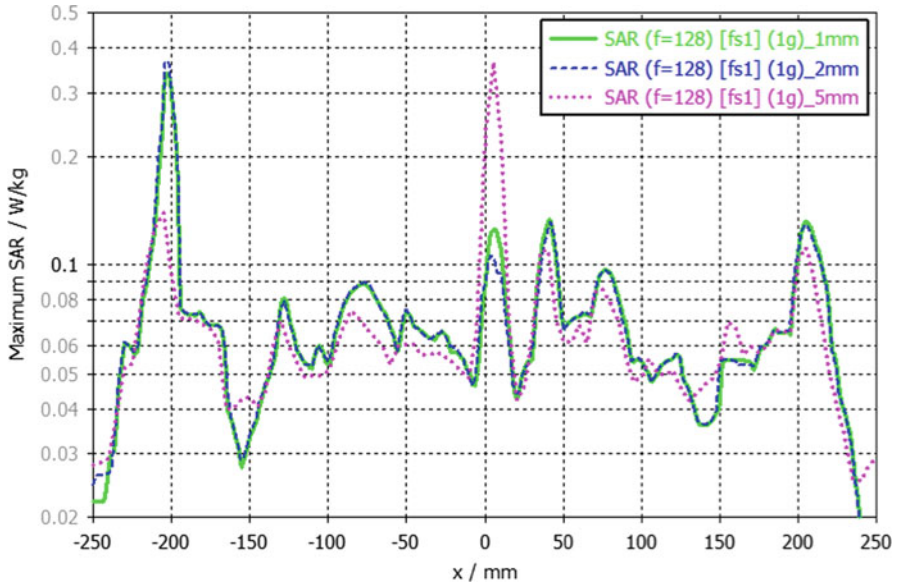


Fig. 7 SAR profile showing the plane-wise maximum along x

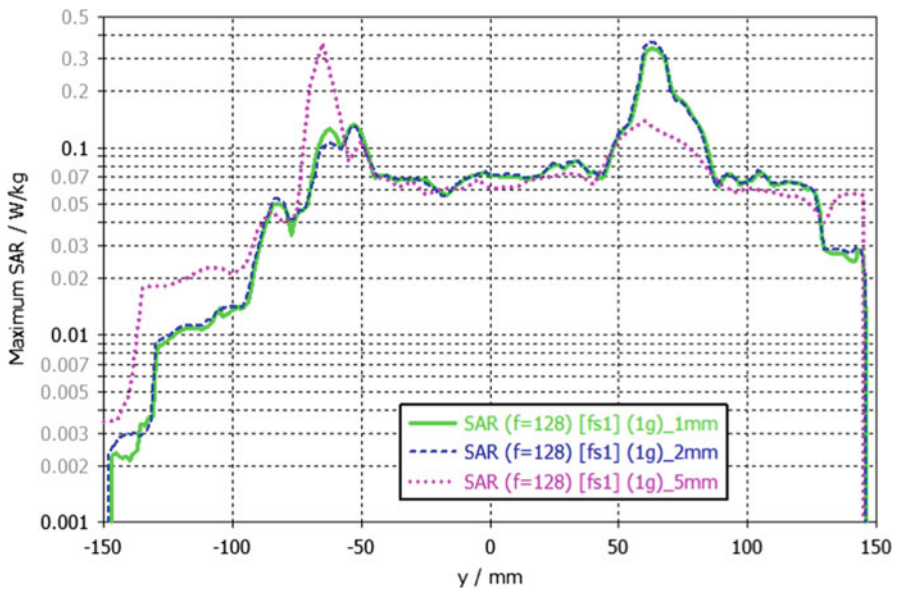


Fig. 8 SAR profile showing the plane-wise maximum along y

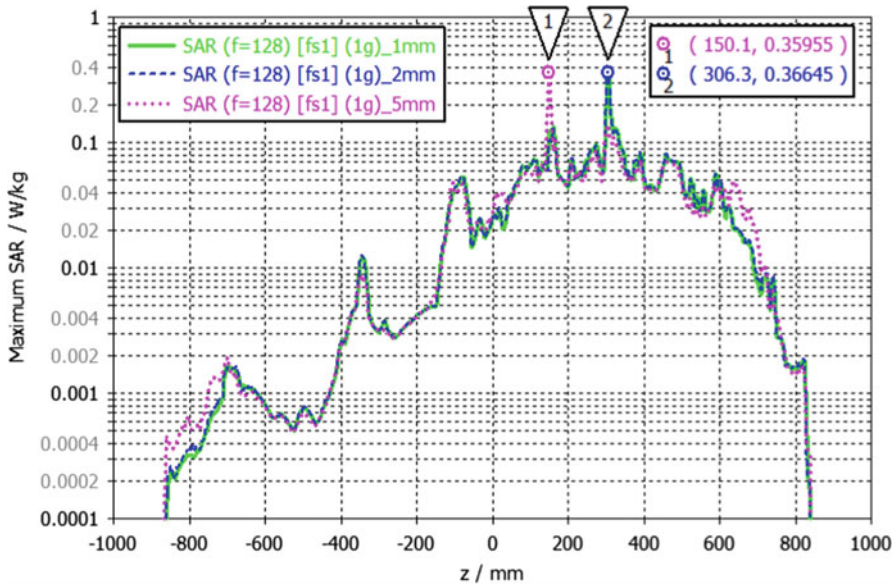


Fig. 9 SAR profile showing the plane-wise maximum along  $z$

the right arm at  $x = -200$ . Such representations can be called SAR profiles and can be helpful for the definition of subvolumes described in 62704-4 to avoid refined sampling in regions with low exposure.

## 5 Conclusion

The investigation shows that good agreement can be achieved, but care needs to be taken when limiting the evaluation on subregions as suggested in clause 6.2.2.2 e) of 62704-4 [2]. The SAR profiles introduced in this work can be of help here. The investigated case suggests that from the initial sampling, the subregion should be chosen at least large enough such that in the excluded regions the SAR profiles are below 10% of the global maximum.

## References

1. IEC/IEEE 62704-1. (2017). Determining the peak spatial-average specific absorption rate (SAR) in the human body from wireless communications devices, 30 MHz to 6 GHz – Part 1: General requirements for using the finite-difference time-domain (FDTD) method for SAR calculations. [www.iec.ch](http://www.iec.ch)



2. IEC/IEEE 62704-4. (2020). Determining the peak spatial-average specific absorption rate (SAR) in the human body from wireless communications devices, 30 MHz to 6 GHz – Part 4: General requirements for using the finite-element method for SAR calculations. [www.iec.ch](http://www.iec.ch)
3. Yanamadala, et al. (2016). Multi-purpose VHP-female version 3.0 cross-platform computational human model. In EuCAP16, Davos, Switzerland, April 2016, pp. 1–5.
4. Massey, J. W., Prokop, A., & Yilmaz, A. E. (2017). A comparison of two anatomical body models derived from the female Visible Human Project data. In: EMBC'17, Jeju Island, Korea, July 2017.
5. Andreuccetti, D., Fossi, R., & Petrucci, C. (1997). An Internet resource for the calculation of the dielectric properties of body tissues in the frequency range 10 Hz–100 GHz. In IFAC-CNR, Florence (Italy). Based on data published by C. Gabriel et al. in 1996. [Online]. Available: <http://niremf.ifac.cnr.it/tissprop/>
6. Prokop, A., Wittig, T., & Levine, S. (2018). Efficient computational investigation of implant RF safety with anatomical human models in MRI systems. In IEEE EMBC, Honolulu, USA, July 2018.

**Open Access** This chapter is licensed under the terms of the Creative Commons Attribution 4.0 International License (<http://creativecommons.org/licenses/by/4.0/>), which permits use, sharing, adaptation, distribution and reproduction in any medium or format, as long as you give appropriate credit to the original author(s) and the source, provide a link to the Creative Commons license and indicate if changes were made.

The images or other third party material in this chapter are included in the chapter's Creative Commons license, unless indicated otherwise in a credit line to the material. If material is not included in the chapter's Creative Commons license and your intended use is not permitted by statutory regulation or exceeds the permitted use, you will need to obtain permission directly from the copyright holder.

